

## Study of Pitting Corrosion Behavior of FSW weldments of AA6101- T6 Aluminium Alloy

L.V. Kamble<sup>1</sup>, S.N. Soman<sup>2</sup>, P.K. Brahmkar<sup>3</sup>, V.V. Mathane<sup>4</sup>

<sup>1</sup>(Mechanical Engineering Department, The M. S. University of Baroda, India)

<sup>2,4</sup>(Metallurgical and Materials Engineering Department, The M. S. University of Baroda, India)

<sup>3</sup>(Mechanical Engineering Department, Dr. Babasaheb Ambedkar Technological University, Lonere, India)

### ABSTRACT

Friction Stir Welding (FSW) is a promising solid state joining process widely used generally for Al alloys, especially in aerospace, marine and automobile applications. In present work, the microstructure and corrosion behavior of friction stir welded AA6101 T6 Al alloy is studied. The friction stir welding was carried using vertical milling machine with different tool rotational speeds and welding speeds. The microstructure at weld nugget or stir zone (SN), thermo-mechanically affected zone (TMAZ), heat affected zone (HAZ) and base metal were observed using optical microscopy. The corrosion tests of base alloy and welded joints were carried out in 3.5% NaCl solution at temperature of 30° C. Corrosion rate and emf were determined using cyclic polarization measurement.

**Key words** - cyclic polarization, friction stir welding, microstructure, nugget, TMAZ.

### I. Introduction

The FSW process is recently applicable for welding of aluminium and magnesium alloys as well as other non-ferrous and ferrous materials as well as composites and dissimilar materials<sup>[1, 2]</sup>. Welding of heat treatable AA6xxx Al alloy by FSW<sup>[3]</sup> gives better quality weld compared to other fusion welding processes. Since there is no direct melting involved, the control needed in fusion welding (to avoid phenomenon like solidification and porosity, loss of volatile solutes) can be avoided in this process. The solid state joining has led to attempt FSW for a wide range of alloys<sup>[4-6]</sup>. Recently aluminium alloys are used in automotive, shipbuilding, aircraft and railway industries, because they are light in weight, easy to machine and have relatively high strength properties. Age hardening heat treatment (T4 or T6) is used for increasing the strength in heat treated aluminium alloys (2xxx, 6xxx, and 7xxx series). In case of fusion welding processes such as TIG or MIG hot cracking observed. These problems can be eliminated in FSW<sup>[7]</sup>. Wert [2003]<sup>[8]</sup> studied FSW of AA2024 welded with aluminium matrix composite and observed grain boundary liquation cracking on 2024 side of the weld. The 2024 T3 Al alloy is widely used as a structural material of aircraft. But it is susceptible to localized corrosion such as pitting. Generally temperature, humidity and salinity are the main factors considered for the accelerated test.

Venugopal et al [2004]<sup>[9]</sup> studied microstructures and pitting corrosion properties of FSW of AA7075 Al alloy in 3.5%NaCl solution. Corrosion resistance of weldments at TMAZ is better than base metal. Friction stir welding of 7075 alloy resulted in fine

recrystallized grains in a nugget which had been attributed from frictional heating and plastic flow of material. Cao and Kou [2005]<sup>[10]</sup> studied FSW, GMAW of AA2219 alloy. GMAW was conducted to provide a benchmark for checking liquation in FSW of 2219 alloy. The microstructures of the resulting welds were examined by both optical microscope and SEM and were found that in GMAW of 2219 alloy Al<sub>2</sub>Cu particles act as in-situ micro sensors clearly in decanting the onset of liquation and show no evidence of induced liquation during FSW.

Ju Kang et al<sup>[11]</sup> investigated the surface corrosion behavior of AA2024-T3 Al alloy sheet welded by FSW by using in-situ observation method. From the SEM observation it is found that density and degree of pitting corrosion in the shoulder active zone was slightly larger compared to other regions on the top surface. The origin of the pitting corrosion was in the region between the  $\delta$ -phase particles and the adjacent aluminium base.

The objective of the present work is to undertake the relationship between the microstructure in various zones and the corrosion behavior.

### II. Friction stir welding process

In FSW, a rotating tool-shoulder & pin or pin with non rotating shoulder generate heat by friction and rotation and stir the faying surfaces to produce intermingling at atomic scale that result in sound welds.

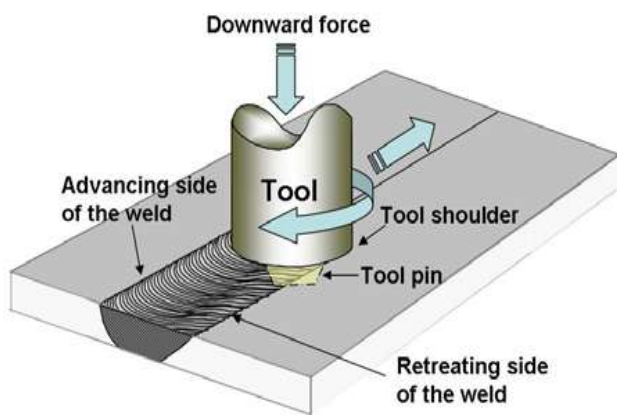


Fig. 1: Basics of Friction Stir Welding

A rotating tool is pressed against the surface of two abutting or overlapping plates. Frictional heat is generated, principally due to the high normal pressure and shearing action of the shoulder. Friction stir welding can be thought of as a process of constrained extrusion under the action of the tool. The frictional heating causes a material to plasticize and form around the probe. Due to tool shoulder this softened material cannot escape out. As the tool is traversed along the joint line, material is swept around the tool probe between the retreating side of the tool and the surrounding unreformed material. The extruded material is deposited to form a solid phase joint behind the tool.

### III. Experimental Work

The main objective of this work is to study the microstructure and corrosion behavior of friction stir welding of Al alloy. For this purpose the plates of 6 mm thickness AA6101 aluminium alloy were cut into size 100 mm x 100 mm and machined with square butt joint configuration. The initial configuration was obtained by securing the plates in butt position using specially designed and fabricated fixture. The welding was carried out in normal to the rolling direction in a single pass using non-consumable tool made of EN24 steel. The chemical composition of the AA6101-T6 material is given in Table (1).

Table (1): Chemical composition of AA 6101-T6

Elements	%
Al	Balance
Mg	0.6
Si	0.5
Zn	0.021
Cu	0.074
Cr	0.015

An indigenously modified machine setup was used for FSW in the present study. The welding parameters namely rotational speed (rpm) and

traverse speed (welding speed) selected for this experimentation are based on the literature review and entire work which was carried out on this alloy. The welding parameters and tool dimensions are given in Table (2).

Table (2): Welding parameters and Tool dimensions

Process parameters and tool details	Values
Rotational speed (rpm)	545, 765, 1070
Welding speed (mm/min)	50, 78, 120
D/d ratio of tool	3.0
Tool shoulder diameter, D (mm)	18.0
Pin diameter, d (mm)	6.0
Tool tilt angle (°)	0.0

For the microstructure analysis, the samples were cut into the required size of pieces. The section was taken across the welding direction. Then the samples were prepared as per standard metallographic process. The sample was then etched using 4M Keller's reagent for 1 to 3 min<sup>[12]</sup>. After etching the microstructure studies were conducted to identify different zones of stir welding samples, with the help of Neophot 2 and SEM (scanning Electron Microscope) at 250X magnification.

### 3.1 Corrosion Studies

Polarization studies were carried out using potentiostate supported with software and the scan rate and potential range for the scan was finalized on the basis of OCP of the material. Scan rate defines the speed of the potential sweep in mV/sec. in this range the current density v/s voltage curve was almost linear. A linear data fitting of the standard model gives an estimate of the polarization resistance, which is used to calculate the corrosion current density  $I_{corr}$  and corrosion rate<sup>[13]</sup>. The tests were performed using MYGAMRY software. Studies were carried out AA6101-T6 Al alloy and FS welded samples were used as working electrode (WE), a saturated calomel electrode immersed in the salt solution was used as reference electrode (RE), and a carbon electrode was used as an auxiliary electrode (AE).

Samples were prepared carefully having 0.25 cm<sup>2</sup> area and using exposure window exposed to 3.5% NaCl solution over the TMAZ and HAZ of weld joint and base metal. The potentiodynamic scan was performed with scan rate of 10mV/sec using potentiostate supported by corrosion measuring software.

## IV. Results and Discussion

The FSW results into generation of the microstructure of friction stir welded joint which is totally different from base metal. These changes

occurred lead to different corrosion behavior of the weld. FSW is essentially a hot working process, where a large amount of deformation is induced into the work piece due to heat and the flow of material caused by active participation of shoulder and probe of the FSW tool.

#### 4.1 Microstructural observations

Principally Four zones are found to be developing in FSW viz, (i) Stir nugget (SN), or stir zone (SZ), which fully recrystallized region at the weld centre. (ii) Thermo-mechanically affected zone (TMAZ), which is affected by heat and deformation, but no recrystallization. (iii) Heat affected zone (HAZ), which is affected by only heat with no plastic deformation. (iv) Base metal. Fig.2 shows the microstructure at the cross section area of welded

joint. The microstructure of stirred zone consists of equated grains in much smaller size compared to the large elongated grains of base metal.

The recrystallized grain structure at the centre position of the stirred zone shows two different microstructures. The first is a fine grain region at the left side resulted from the action of rotating probe. The second is an elongated microstructure at the right side remaining from the base metal. The transition region between the weld nugget and TMAZ is clearly observed as being microscopically sharp described as adjacent to the fully recrystallized nugget containing grains that exhibit varying degree of recovery and recrystallization to give equiaxed grains. Microstructure of heat affected zone (HAZ) and base metal are distinctly seen.

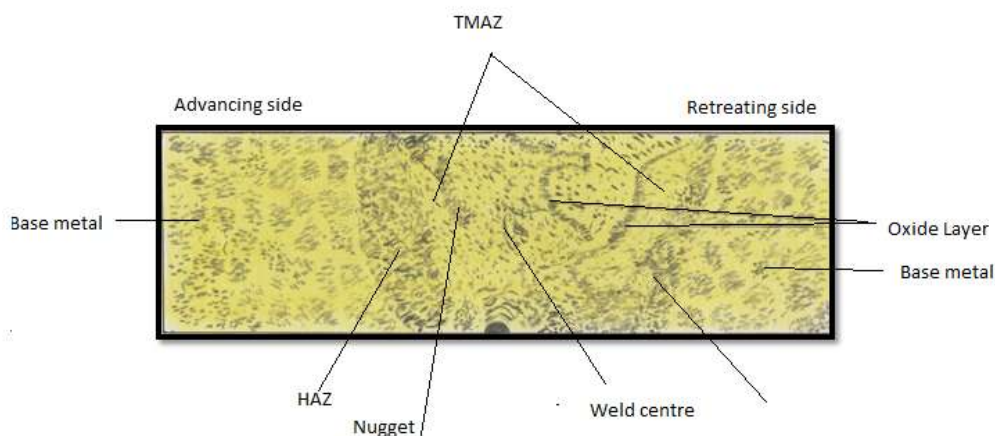


Fig. 2: Micro structural zones of sample E1

From the microstructure study of AA 6101 aluminum alloy which was welded using friction stir welding technique. Based on microstructure observation identification of various zone is carried out. It was found that the nugget comprise of the onion ring structure with fine equiaxed grains with heavy density precipitates. The microstructure comprises more coarse grains of Al.

The TMAZ, it is the zone characterized with the gradient of the plastic strain and the temperature. In this zone there is no stirring action takes place, the material deform with increase in the temperature. The level of deformation is less compare to weld centre region. It consist of fine grains of Al with the presence of ripen precipitates of the  $Mg_2Si$  there is also formation of precipitates free zone.

In the HAZ there is only temperature gradient exists. So it consists of the coarse grain structure with presence of  $Mg_2Si$  precipitates. There was also some precipitates free zone in the HAZ. With increase in

the tool rotation speed and welding speed the grain refinement was observed in HAZ either at advancing side or at retreating side. At tool rotation speed of 1070 rpm the grain refinement was observed in HAZ of both side that is an advancing side as well as at retreating side.

#### 4.2 Corrosion observations

A passive oxide film generally developed readily on the aluminium alloys, when exposed to air or water. However the corrosion rate could be very high due to the presence of chloride ion <sup>[14]</sup>. Further the corrosion behavior of Al alloys largely depends on heterogeneity of their microstructures. In this study, electrochemical corrosion test was carried out by Cyclic Polarization of base metal and the FSW welded samples of AA6101-T6 alloy using 3.5% NaCl solution, corrosion potential ( $E_{corr}$ ) and corrosion current ( $I_{corr}$ ) are also evaluated. The measured values are shown in Table (4).

**Table (4):** Result of Cyclic Polarization Experiments

Sample code	$I_{corr}$ ( $\mu A$ )	$E_{corr}$ (mV)	$E_{pit}$ (mV)	Corrosion rate (mpy)
Base metal	0.067	-600.0	-842.8	115.0e-3
E1-T	0.156	-804.0	-866.9	267.2e-3
E2-T	1.090	-762.0	-861.9	1.877
E3-T	0.933	-724.0	-827.9	1.704
H1-T	0.639	-1180.0	-821.2	1.097
H2-T	75.20	-710.0	-944.3	129.1
H3-T	0.128	-723.0	-820.4	219.2e-3
M1-T	0.0858	-767.0	-934.4	147.1e-3
M2-T	0.255	-737.0	-917.2	437.8e-3
M3-T	1.080	-768.0	-848.4	1.852
E1-H	0.430	-1040.0	-838.7	737.7e-3
E2-H	2.060	-822.0	-883.3	3.538
E3-H	3.610	-783.0	-829.6	6.198
H1-H	0.461	-830.0	-931.9	790.2e-3
H2-H	0.605	-1010.0	-865.1	1.038
H3-H	1.300	-733.0	-813.9	2.238
M1-H	0.214	-858.0	-831.1	366.4e-3
M2-H	0.227	-932.0	-880.6	390.0e-3
M3-H	0.411	-1000.0	-854.0	705.7e-3

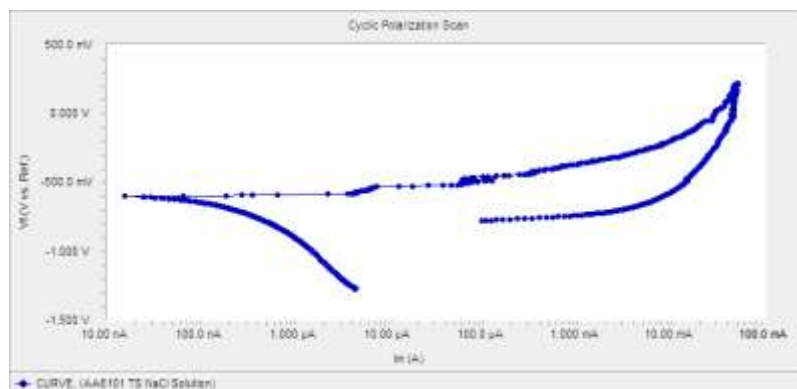


Fig 3: Cyclic polarization curve for base metal in 3.5%NaCl

Observations of the welded samples

1. The cyclic polarization curve of base metal having grade AA 6101 T6 aluminum alloy was obtained by performing cyclic polarization test on given base metal in 3.5%NaCl environment. The curve obtained shows positive hysteresis Fig.3.

Also here  $E_{pit} < E_{corr}$  which indicate that pitting will occur and damage passive film which is not repairable and it will further corroded under pitting manner.

The observations for TMAZ are given below as per curve obtained in Fig. 4A.

2. The cyclic polarization curve for E1-T, E2-T, E3-T of FSW joint shows positive hysteresis.

Also here  $E_{pit} < E_{corr}$  which indicates that pitting will occur and damage passive film which is not repairable and it will further corroded under pitting manner.

3. The cyclic polarization curve of H1-T FS welded sample shows negative hysteresis.

Also here  $E_{pit} > E_{corr}$  which indicates that pitting will occur but in passive zone and damage passive film can be repaired and it will prevent further corrosion.

4. The cyclic polarization curve of H2-T, H3-T, M1-T, M2-T and M3-T FSW shows positive hysteresis.

Also here  $E_{pit} < E_{corr}$  which indicates that pitting will occur and damage passive film which is not repairable and it will further corroded under pitting manner.

Similar study was conducted and the observations are given as below for Heat affected zone (H). Fig. 4B

1. The cyclic polarization curve of E1-H FSW welded shows negative hysteresis.

Also here  $E_{pit} > E_{corr}$  which indicate that pitting will occur but in passive zone and damaged passive

film can be repaired and it will prevent further corrosion.

2. The cyclic polarization curve of E2-H, E3-H, H1-H, H3-H, shows positive hysteresis. Also here  $E_{pit} < E_{corr}$  which indicate that pitting will occur and damaged passive film which is not repairable and it will further corroded under pitting manner.
3. The cyclic polarization curve of H2-H FSW welded shows negative hysteresis. Also here  $E_{pit} > E_{corr}$  which indicate that pitting will occur but in passive zone and damage passive film can be repaired and it will prevent further corrosion.
4. The cyclic polarization curve of M1-H, M2-H, M3-H FSW welded shows negative hysteresis. Also here  $E_{pit} > E_{corr}$  which indicate that pitting will occur but in passive zone and damaged passive film can be repaired and it will prevent further corrosion.

## V. Conclusions

From the experiment we can draw the following conclusions-

1. FSW welding results into formation of distinguished zones namely nugget, TMAZ, HAZ.
2. HAZ (heat affected zones) and TMAZ (thermo mechanically affected zones) are of more of the interest as they incorporate the most thermal and mechanical stress which make them most likely to be attacked by environment.
3. In case of HAZ the passivity film may be or may not be repairable, it depends on the heat input & extent of heat distribution.
4. From cyclic polarization studies,
  - a. The potentiodynamic polarization curve having negative hysteresis loop, makes the sample corrosion resistant.
  - b. The potentiodynamic polarization curve having positive hysteresis loop, results into tendency of pitting, which continuously grow.
5. Among all the samples welded with rotational speed of 1070 rpm shows pitting resistance. (M1-H, M2-H, M3-H)
6. From overall observation, it can also be concluded that at all rotational speed and at low welding speed, pitting resistance is observed. (E1-H, H1-T, H1-H, M1-T, M1-H)
7. In general high rotational & low welding speed results into less distorted HAZ & TMAZ and hence better pitting resistance.

## VI. Acknowledgement

My heartfelt thanks to Dr. K.B. Pai, former Head of Metallurgical and Materials Engineering

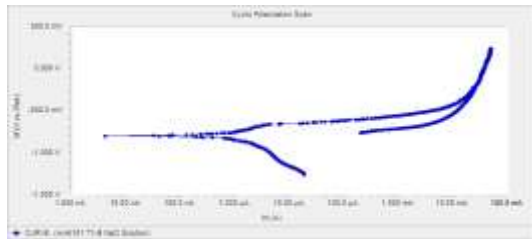
Department, The M. S. University of Baroda for providing financial support under UGC XI plan.

## References

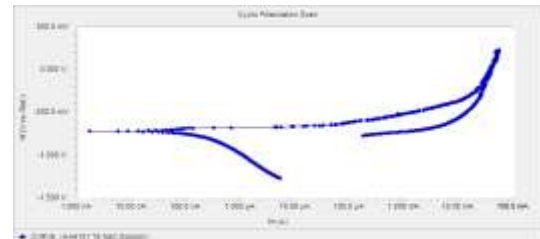
- [1] R. Rai, A. De, H. K. D. H. Bhadesia and T. DebRoy, Review: friction stir welding tools, *Science and Technology of Welding and Joining*, 16(4) 2011, 335-341.
- [2] H. Uzun, C. D. Donne, A. Argagnotto, T. Ghidini and C. Gambaro, Friction stir welding of dissimilar Al6013-T4 to X5CrNi18-10 stainless steel, *Materials and Design*, 26, 2005, 41-16.
- [3] C. Hamilton, S. Dymek, and M. Blicharski, Mechanical properties of al 6101-T6 welds by friction stir welding and metal inert gas welding, *Archives of Metallurgy and Materials*, 52, 2007, 67-72.
- [4] R. Nandan, T. DebRoy and H.K.D.Bhadesis, Recent Advances in Friction Stir Welding Process, weldment structure and properties, *Progress in Materials Science*, 53, 2008, 980-1023.
- [5] Maria Posada, Jennifer P. Nguyen, David R. Forest, Jobnnie J. Branch, Robert Denale, Friction Stir Welding Advanced Joining Technology, special issue, AMPIAG, Quarterly vol 7, no. 3, 2003, 13-20.
- [6] Sindo Kou, *Welding Metallurgy*, 2<sup>nd</sup> edition, John Wiley and Sons, Inc. Publication, USA, 2003.
- [7] Takenori Hashimoto et al, FSW joints of High Strength Al Alloy, 1<sup>st</sup> International Symposium on Friction Stir Welding, 14-16 june, 1999, Osaka, CA, USA.
- [8] Wert J.A., Microstructures of Friction Stir Weld joints between Aluminium base metal matrix composite and A monolithic Al Alloy, *Scripta Materials*, 49,2003, 607-612.
- [9] Venugopal T, Srinivas Rao K, Prasad Rao K, Studies on Friction Stir Welding of AA7075 Al Alloy, *Trans Indian Inst. Met*, Vol 57, no.6, 2004, 659-663.
- [10] Cao G, Kou S, Friction Stir Welding of 2219 Aluminium Behavior of Al<sub>2</sub>Cu particles, *Suppliment of Welding Journal*, January 2005, pp 1S-8S.
- [11] Ju Kang, Rui -dong Fu, Guo-hong Luan, Chun-lin Dong, Miao He, In -situ Investigation on the Pitting Corrosion Behavior of
- [12] ASM handbook for Metallography and microstructure, vol 9, page no 1720.
- [13] David G. Enos, The Potentiodynamic Polarisation Scan, Technical Report 33, University of Virginia, 1997.

Friction Stir Welded joint of AA2024-T3 Aluminium Alloy, *Corrosion Science*, vol.52, 20120, p 620-626.

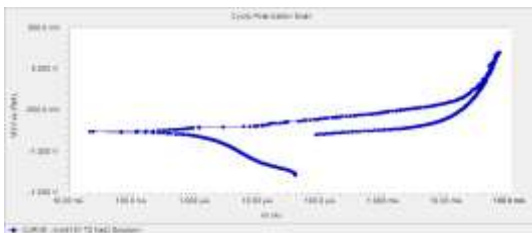
[14] Kenneth R. Trethewey, Chamberlain J, *Corrosion for Science and Engineering*, Longman Group Limited, 2<sup>nd</sup> Edition, 1996.



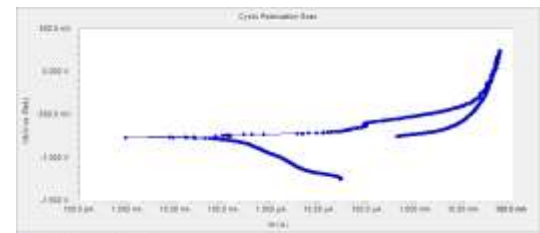
(a): Cyclic polarization curve for E1-T



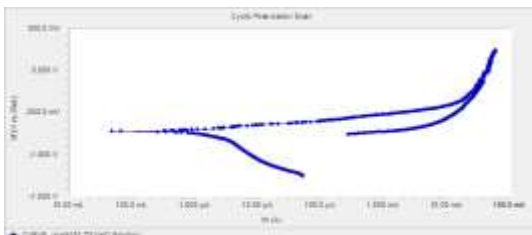
(f): Cyclic polarization curve for H3-T



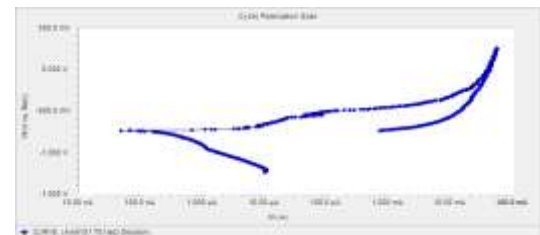
(b): Cyclic polarization curve for E2-T



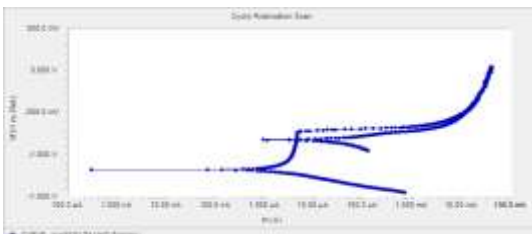
(g): Cyclic polarization curve for M1-T



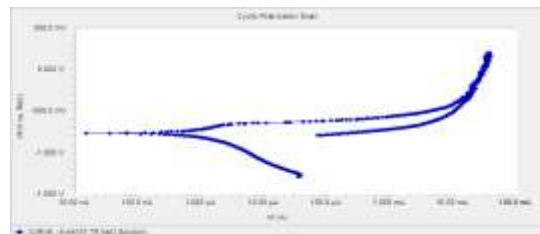
(c): Cyclic polarization curve for E3-T



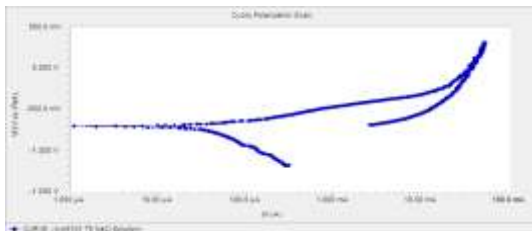
(h): Cyclic polarization curve for M2-T



(d): Cyclic polarization curve for H1-T

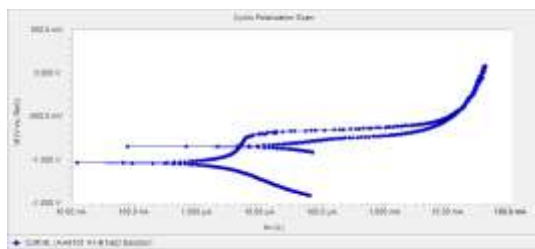


(i): Cyclic polarization curve for M3-T

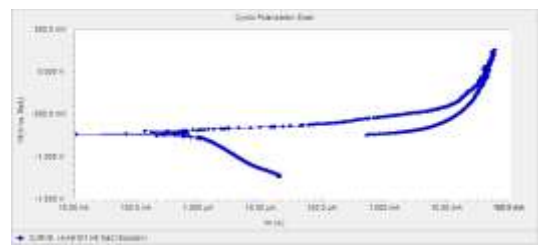


(e): Cyclic polarization curve for H2-T

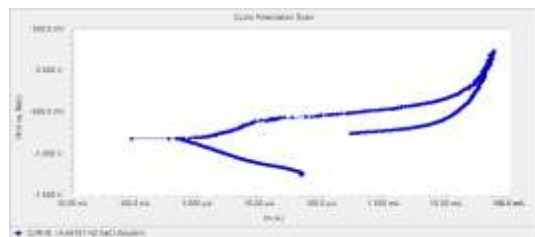
Fig. 4A: Cyclic polarization curve for TMAZ in 3.5%NaCl



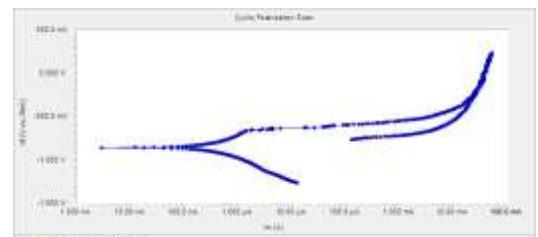
(1): Cyclic polarization curve for E1-H



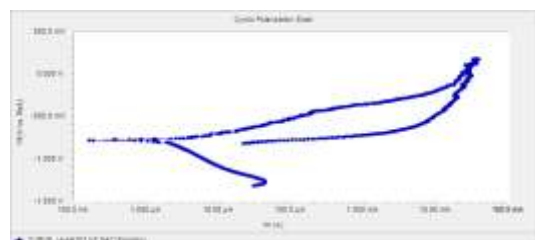
(6): Cyclic polarization curve for H3-H



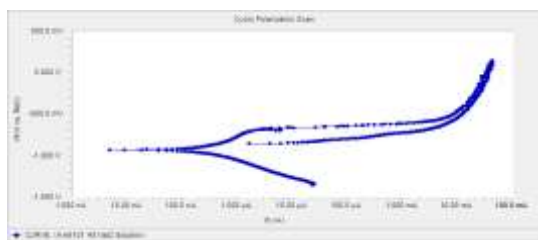
(2): Cyclic polarization curve for E2-H



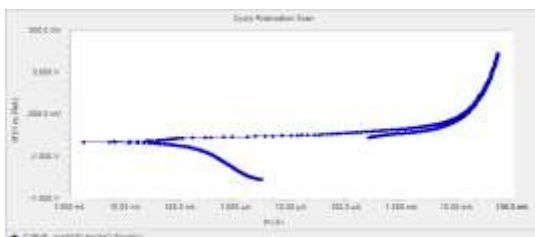
(7): Cyclic polarization curve for M1-H



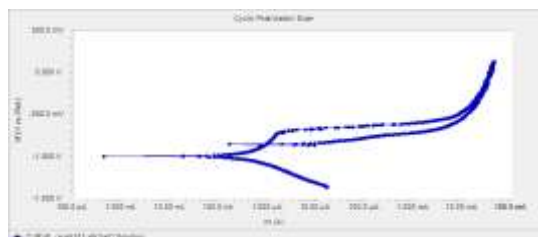
(3): Cyclic polarization curve for E3-H



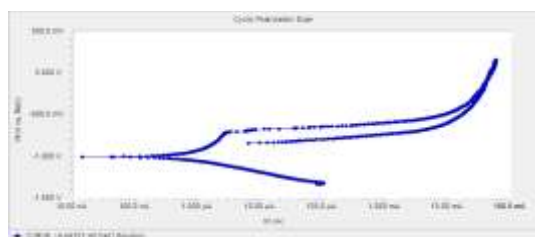
(8): Cyclic polarization curve for M2-H



(4): Cyclic polarization curve for H1-H



(9): Cyclic polarization curve for M3-H



(5): Cyclic polarization curve for H2-H

Fig. 4B: Cyclic polarization curve for HAZ in 3.5%Nacl